RESEARCH ARTICLE
doi: 10.2306/scienceasia1513-1874.2022.142

ScienceAsia 49 (2023): **131–140**

Geology, mineralization, and alteration of B Prospect of the epithermal Au-Ag deposit in Central Thailand: A study on Chatree's satellite deposit for future gold exploration

Sirawit Kaewpaluk[a], **Abhisit Salam**[a,*], **Thitiphan Assawincharoenkij**[a,b], **Takayuki Manaka**[c], **Sopit Poompuang**[a], **Surachat Munsamai**[d], **Khin Zaw**[e]

[a] Department of Geology, Faculty of Science, Chulalongkorn University, Bangkok 10330 Thailand
[b] Applied Mineral and Petrology of Special Task Force for Activating Research (AMP STAR), Department of Geology, Faculty of Science, Chulalongkorn University, Bangkok 10330 Thailand
[c] Institute for Geo-Resources and Environment, Geological Survey of Japan, National Institute of Advanced Industrial Science and Technology (AIST), Tsukuba, Ibaraki 305-8567 Japan
[d] Akara Resources Public Company Limited, Thap Khlo, Phichit 66230 Thailand
[e] CODES ARC Centre of Excellence in Ore Deposits, University of Tasmania, Hobart, Tasmania 7001 Australia

*Corresponding author, e-mail: abhisit.a@chula.ac.th

Received 19 Sep 2021, Accepted 19 Aug 2022
Available online 25 Oct 2022

ABSTRACT: The B prospect is located at the southeast of the Chatree gold-silver deposit. The mineralization is hosted in the Late Permian-Early Triassic Chatree volcanic sequence consisting of volcaniclastic and volcanogenic-sedimentary rocks ranging in composition from basaltic andesite to rhyolite. At the study area, the total thickness of volcanic succession is about 300 meters, and the succession can be divided into 3 main stratigraphic units from bottom to top, namely 1) porphyritic andesite unit (Unit 3), 2) polymictic intermediate breccia unit (Unit 2), and 3) volcanogenic sedimentary unit (Unit 1). The ore zones are mainly confined to polymictic intermediate breccia and volcanogenic sedimentary units (Unit 1 and 2). At least 3 stages of mineralization have been identified, namely 1) quartz-pyrite (Stage 1), 2) quartz-chlorite-calcite-sulfide-electrum (Stage 2), and 3) quartz-calcite (Stage 3) veins/veinlets. Gold occurs chiefly in Stage 2 mineralization which is characterized by typical vein textures of low sulfidation epithermal deposit (e.g., crustiform, colloform banding, and comb textures). Pyrite is the primary sulfide mineral with minor sphalerite, chalcopyrite, and galena. Gold occurs as electrum with fineness ranging from 506 to 632. The hydrothermal alteration at B prospect is composed of 2 main types: (1) quartz-adularia (silicic alteration) assemblage close to ore zone and (2) adularia-quartz-illite-calcite-chlorite (phyllic alteration) assemblage distal to ore zone. Based on characteristics of mineral assemblages, textures, and alterations, the mineralization at B prospect can be classified as a low sulfidation epithermal gold-silver style deposit.

KEYWORDS: B prospect, epithermal, low sulfidation, gold, mineralization, mineral

INTRODUCTION

Several gold deposits are situated in the Loei Fold Belt (LFB), Thailand [1, 2] (Fig. S1a). Along the LFB, Chatree gold-silver deposit [2–5] located in Phetchabun and Phichit Provinces [6–9] (Fig. S1a and b) has the largest gold resources and is surrounded by several satellite deposits which are currently recognized for future potentials such as Suwan [10], Chokdee, and B prospects. Of these, the B prospect located at 3 km south of the Chatree deposit (Fig. S1c) is the nearest prospect and has high economic interest in terms of exploration perspective with the best assay result including 50 m at 7.0 g/t Au, 70 m at 2.0 g/t Au, and 110 m at 1.8 g/t Au [11]. This prospect is situated on the similar structure (NNW-SSE trending fault) which hosts the main ore lenses at the Chatree deposit [4] and Suwan prospect [10]. However, the B prospect is still in prospect status and thus no detailed study has been undertaken on this prospect area. Therefore, this study was conducted aiming to investigate the comprehensive geological characteristics (geology and mineral chemistry) of the B prospect and the relationship between the B prospect, Suwan prospect, and Chatree deposit to establish a deposit model which will be applicable for further gold exploration in the surrounded area of the Chatree deposit.

Geological setting

Thailand comprises 2 major tectonic terranes: Sibumasu Terrane in the west and Indochina Terrane in the east (Fig. S1a) [2, 12–14]. The subduction and collision between the Sibumasu and Indochina Terranes during Permo-Triassic period have established 2 parallel igneous belts along their margins, namely Sukhothai Arc (or Sukhothai Fold Belt) in the west and LFB in the east [2, 7]. The LFB extends from Lao PDR along with the western edge of the Khorat Plateau in Thailand and through to western Cambodia. This fold belt is one of the most important mineral belts in Thailand particularly for gold, silver, and copper resources [2]. There are several gold skarn and epithermal deposits along this belt (Fig. S1a) such as Phu

Lon prospect (Cu-Fe-Au skarn) [1], Puthep prospect (Cu-Au skarn) [15, 16], Phu Thap Fah deposit (Au skarn) [17–20], Wang Yai prospect (low sulfidation epithermal Au-Ag) [21], Khao Phanom Pha deposit (Au skarn), Chatree deposit (low sulfidation epithermal) [1–8], and French mine deposit (Cu-Au skarn) [22]. Of these, the Chatree deposit has been recognized as the largest gold-silver deposit in Thailand in terms of mineral resources (188 Mt at 0.66 g/t Au and 5.42 g/t Ag as of 2013, containing 4.0 Moz gold and 33 Moz silver) [11].

Geology and mineralization of the Chatree deposit

The basement of the host rock sequence at the Chatree deposit is a Carboniferous sedimentary unit and Permian limestone of Saraburi Group [4] which is exposed in the eastern part of the deposit area (Fig. S1b). The host rock sequence of the Chatree deposit dominantly comprises Late Permian-Early Triassic volcaniclastic and volcanogenic sedimentary rocks which are confined to be 260 to 240 Ma ages based on the LA-ICPMS zircon U-Pb dating results [7]. This volcanic sequence is widely distributed in the area with a radius of >20 km from the Chatree deposit [4], and therefore host rock sequence at the B prospect is a part of the host sequence at the Chatree deposit as well (Fig. S1b). The total thickness of the entire volcanic sequence of the Chatree deposit is at least 550 m [4].

Furthermore, several intrusive units (Fig. S1b) of different ages are distributed around the Chatree deposit area. They are Carboniferous pink granite at Dong Khui Sub-district (Chon Daen District, Phetchabun Province), Early Triassic granite at Wang Pong Sub-district (Wang Pong District, Phetchabun Province), and diorite porphyry at N prospect (Phichit Province) [4, 7, 8].

The Chatree deposit has 2 main structures including the NE-SW and NNW-SSE faults [4, 9], and gold-silver mineralization of the Chatree deposit occurs along the intersection of 2 faults recognized as the main ore zones including Q, A, D, H, C, K-east, and K-west ore lenses (Fig. S1c) [4]. The gold-silver mineralization occurs as veins/veinlets with minor breccia, and they are dominantly hosted in the polymictic mafic-intermediate breccia unit [4, 5, 7]. The mineralized veins commonly show crustiform, colloform, and comb textures with the alternating bands of sulfides. These vein textures are recognized to be the typical features of epithermal style veins [4, 23, 24]. Salam [4] interpreted the vein paragenesis of the Chatree deposit into 3 main stages: pre-, main-, and post-gold-silver mineralization stages. The pre-gold-silver mineralization stage consists of microcrystalline quartz + pyrite vein (Stage 1), quartz-chlorite-sericite-pyrite vein (Stage 2A), quartz-sericite ± chlorite-chalcopyrite-pyrite-sphalerite ± galena vein (Stage 2B), and quartz-carbonate-(K-feldspar) ± carbonate ± sulfides vein (Stage 3). The main gold-silver mineralization stage comprises quartz-chlorite-adularia ± carbonate-sulfide-electrum vein (Stage 4A), quartz ± carbonate-adularia-sulfide-electrum vein (Stage 4B), and carbonate ± quartz-adularia-sulfide-electrum-argentite-tetrahedrite vein (Stage 4C). The post-gold-silver mineralization stage includes quartz ± carbonate vein (Stage 5), quartz ± carbonate vein/veinlet (Stage 6), and quartz-zeolite-carbonate vein (Stage 7). Based on field geology, vein textures, and mineral assemblages, the Chatree deposit is defined as a low sulfidation epithermal gold-silver deposit [4].

MATERIALS AND METHODS

Drilled core logging, sample collection, and petrographic study

This study was conducted fundamentally using drill core samples from 4562DD, 4564DD, and 4576DD drill holes (Fig. 1), which represent main E-W section of the B prospect and show the host volcanic succession and mineralization of the prospect. Diamond cores of the drill holes were logged and correlated to establish the geological cross-section (section no. 1800085mN; Fig. 1). In case of vein samples, they were examined for cross-cutting and overprinting relationships to define the vein stage of paragenesis.

The collection of drill core samples was carried out with a specific focus on the distance between wallrock and vein. For wallrock samples, they were collected from the unaltered, least altered, and altered wallrocks to investigate the rock type and alteration phases. The vein samples were collected in each paragenesis stage to determine the mineral assemblage and vein textures. As a result of sampling work, 20 vein and 16 wallrock samples were obtained and selected to study petrography and mineral chemistry. The petrographic study was conducted using a transmitted light microscope for rock identification and a reflected light microscope (Nikon Polarizing Microscope ECLIPSE lV100N POL, Nikon Metrology, Belgium) for ore petrological study.

Electron probe microanalyzer (EPMA)

Electron probe micro-analyzer (EPMA), JEOL model JXA 8100 (Jeol, Japan), was utilized for investigating the chemical composition of sulfides and electrum at Department of Geology, Chulalongkorn University (CU), Thailand. The operating condition of EPMA included an accelerating voltage of 15 kV, a beam current of 25 nA, and an electron beam diameter of 1 μm. The pure metal standards of gold and silver were applied for this analysis. Detection limits of Au and Ag are 0.05 wt.%. The chemical composition was used to re-identify the mineral type. In addition, for chemical compositions of electrum, they were calculated and reported as fineness. Fineness is the purity of gold

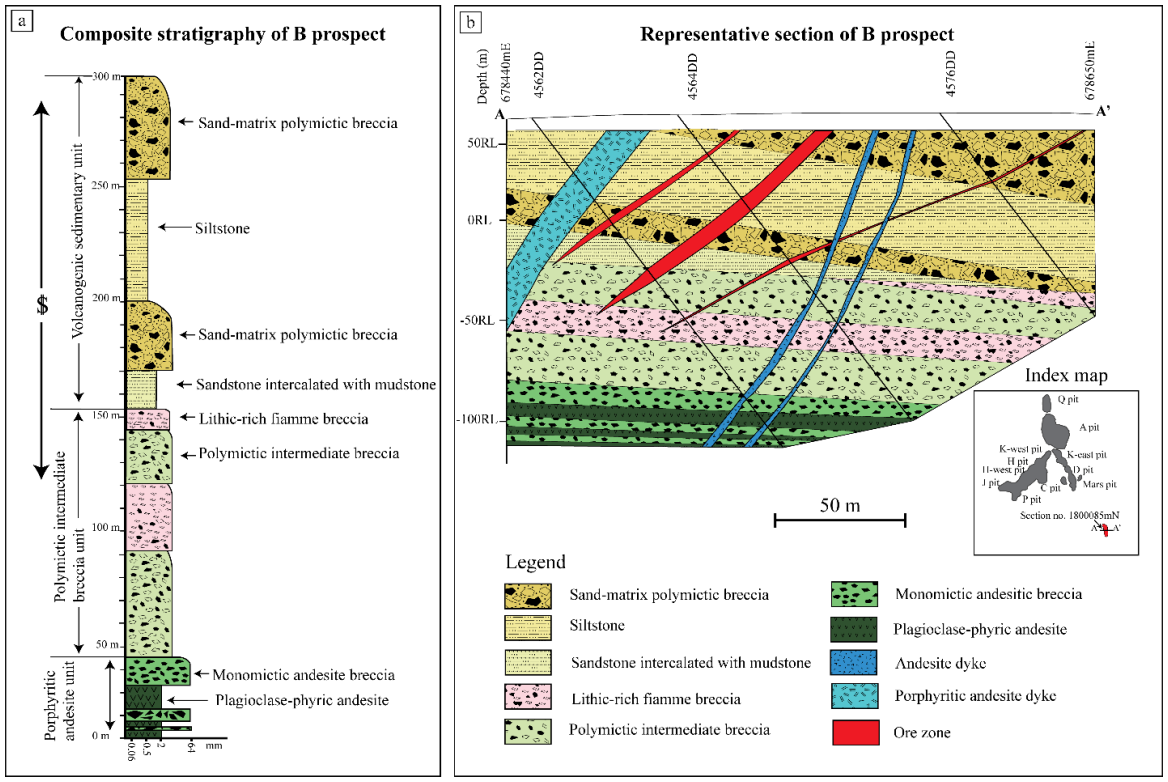

Fig. 1 (a) Composite stratigraphy established from 4562DD, 4564DD, and 4576DD drill holes showing the 3 main units of the B prospect, namely volcanogenic sedimentary unit, polymictic intermediate breccia unit, and porphyritic andesite unit. (b) Representative E-W cross-section of the B prospect (section no. 1800085mN).

which can be calculated by wt.% Au*1000/(wt.% Au + wt.% Ag) [25].

X-Ray diffraction (XRD) analysis

XRD analysis was used to aid in re-identifying alteration minerals. Prior to XRD analysis, the powder samples were prepared, and they were mixed with sodium hexametaphosphate ($(NaPO_3)_6$) and distilled water in a beaker and then leaved overnight. Subsequently, the mixture was stirred gently, dropped on a glass plate, and leaved until dried out. The prepared samples were then analyzed by X-Ray Diffractometer BRUKER model D8 Advance (Bruker, USA) at Department of Geology, Faculty of Science, CU. The XRD analysis was carried out from 5° to 50° 2θ with the operating conditions of 40 kV/30 mA, scan rate 1 s/step, and step 0.02 degree.

RESULTS

Geology of B prospect

The volcanic succession of the B prospect is at least 300 m in thickness (Fig. 1a) and can be divided into 3 main units based on their facies, including rock texture, mineralogy, and composition: (1) porphyritic andesite unit (Unit 3), (2) polymictic intermediate breccia unit (Unit 2), and (3) volcanogenic sedimentary unit (Unit 1), from bottom to top in succession (Fig. 1a and b). The entire volcanic sequence at the B prospect gently dips to the east (Fig. 1b). The established composite stratigraphy and geological cross-section of the B prospect are shown in Fig. 1. The 3 main rock units at the B prospect are described below from bottom to top.

The porphyritic andesite unit, the lowest stratigraphic unit, comprises plagioclase-phyric andesite and monomictic andesitic breccia. Plagioclase-phyric andesite is a coherent rock unit characterized by abundant fine-grained plagioclase with rare hornblende phenocrysts (Fig. 2a and b). This coherent rock unit is commonly intercalated with monomictic andesitic breccia which is composed dominantly of plagioclase-phyric andesite clasts. This unit is overlain by a polymictic intermediate breccia unit with gradational contact. This unit (Unit 2) consists of lithic-rich fiamme breccia and polymictic intermediate breccia. The lithic-rich fiamme breccia comprises several clast types, including volcanic, mudstone, sandstone, and pumice clasts (Fig. 2c). Distinct textural characteristic of this breccia is the presence of flattened and elongated pumice clasts so-called fiamme texture (Fig. 2d). The polymictic intermediate breccia is also composed of similar types of clasts to the lithic-rich fiamme

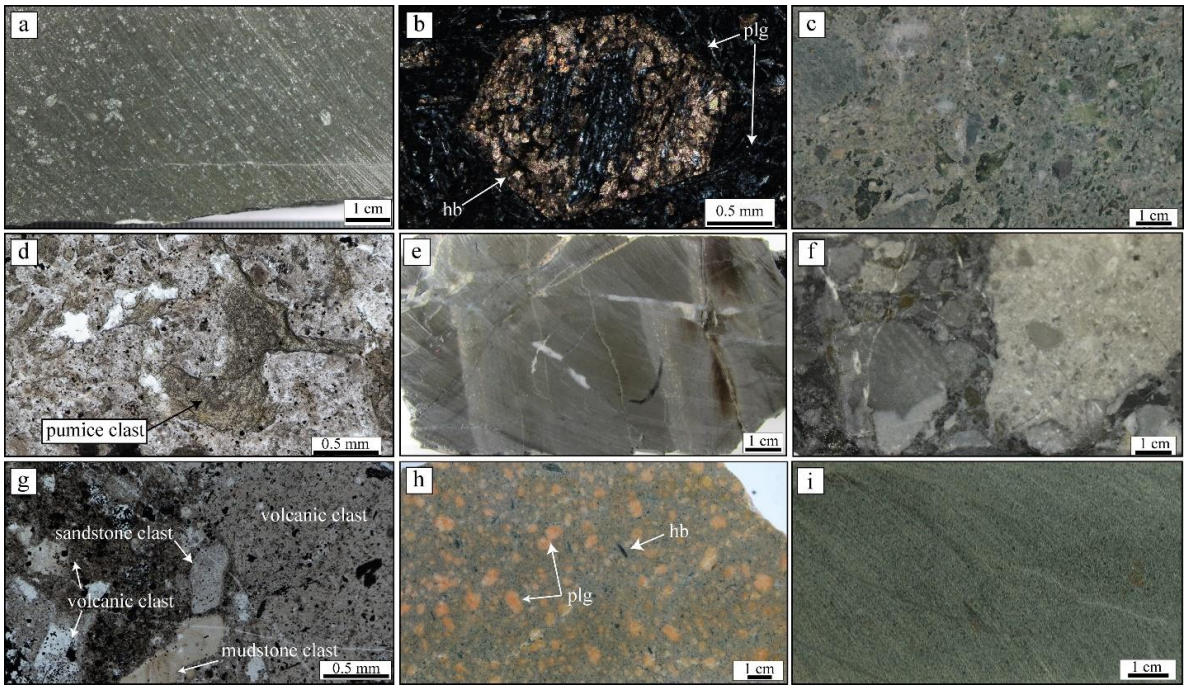

Fig. 2 Representative host rocks of the B prospect. (a) Photograph of plagioclase-phyric andesite in Unit 3. (b) Photomicrograph of plagioclase-phyric andesite showing hornblende phenocryst and fine-grained plagioclase. (c) Photograph of lithic-rich fiamme breccia in Unit 2. (d) Photomicrograph of lithic-rich fiamme breccia showing the elongated pumice clast. (e) Photograph of siltstone in Unit 1. (f) Photograph of sand-matrix polymictic breccia in Unit 1. (g) Photomicrograph of sand-matrix polymictic breccia showing several clasts such as volcanic, sandstone, and mudstone clasts. (h) Photograph of porphyritic andesite dyke. (i) Photograph of andesite dyke. Abbreviations; plg = plagioclase, and hb = hornblende.

breccia, but it involves less abundance of pumice clasts. This unit (Unit 2) is in turn overlain by the volcanogenic sedimentary unit (Unit 1) which is also known as epiclastic rock unit. The contact is gradational contact. It comprises sand-matrix polymictic breccia, siltstone, sandstone, and mudstone. Intercalation of major sandstone and minor mudstone layers is present in the deeper part of this unit. Siltstone consisting of the middle part of this unit shows graded laminations (Fig. 2e). Sand-matrix polymictic breccia forms the top and lower middle parts of the unit (Fig. 2f). It is characterized by several differentiated clasts such as volcanic and sedimentary clasts with poorly sorted sand matrix.

Besides the volcanic sequence, post-mineralization dykes are also identified, and they are classified into 2 types including porphyritic andesite and andesite dykes. These dykes normally strike in N-S direction and with steep westerly dipping geometry and crosscut the whole rock units in the sequence and mineralized veins. The porphyritic andesite dyke is characterized by presence of phenocrysts of orange plagioclase and hornblende crystals (Fig. 2h), while andesite dyke is defined by fine-grained plagioclase and hornblende (Fig. 2i).

Mineralization of B prospect

Ore zone of the B prospect occurs along the NNW-SSE structure which is extended from the Chatree deposit. Results of core logging of the selected drill holes indicate that the ore zone is preferentially hosted in the volcanogenic sedimentary and polymictic intermediate units (Unit 1 and 2; Fig. 1). The ore zone is composed principally of gold-silver mineralization veins/veinlets with minor breccia and stockwork. Based on cross-cutting and overprinting relationships, mineral assemblages, and veins/veinlets textures, the mineralization of the B prospect is divided into 3 stages (Fig. 3). The pre-gold-silver mineralization stage (Stage 1) is defined as quartz-pyrite veins which are characterized by distinct grey quartz with abundant pyrite presenting along rims of veins (Fig. 4a). Pyrite in the grey quartz is occasionally found, and it is normally a euhedral crystal ranging from 0.1 to 0.5 mm in size (Fig. S2a). The pyrite-rich rims of the veins are commonly featured from abundant aggregated pyrite crystals which have a porous texture with an anhedral shape. Stage 2 veins represent the main gold-silver mineralization stage and occur as quartz-chlorite-calcite-sulfide-(pyrite-sphalerite-galena)-electrum vein/veinlet and stockwork (Fig. 4b and c). The distinct textural

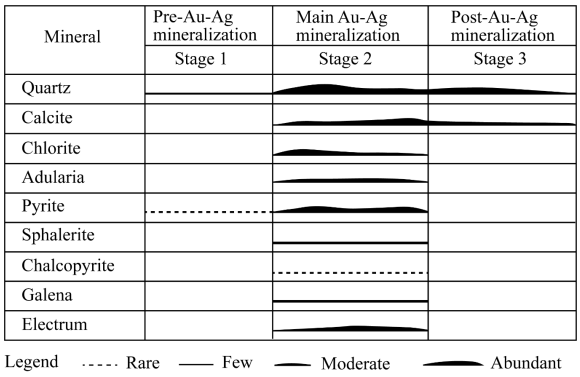

Fig. 3 Paragenesis diagram of the mineralization at the B prospect showing the occurrences and mineral abundance of each mineralization stage.

features of this stage veins are alternating bands of sulfide-rich and quartz-rich layers, which are typically named as crustiform, colloform, and comb textures (Fig. S2b and c). Under microscopic observation, the Stage 2 veins contain pyrite, sphalerite, galena, and electrum in the black bands. The sulfides comprise pyrite, sphalerite, chalcopyrite, and galena (Fig. 3, Fig. 5d, Fig. 5e, and Fig. 5f). Pyrite is the most abundant sulfide in the veins, and it can be separated into 2 types: (1) clean pyrite and (2) porous pyrite (Fig. 4f). Two types of pyrite show crystal sizes ranging from 0.01 to 0.1 mm. Sphalerite, galena, and chalcopyrite are very small for their crystal sizes commonly having 0.005 to 0.02 mm in size, and they often occur as inclusions of pyrite (Fig. 4d and e). Gold occurs as electrum in irregular shapes and is intimately associated with pyrite (Fig. 4f). EPMA spot and imaging analyses of Au and Ag compositions of the electrum grains (Fig. 4g and h) indicate that they have fineness ranging from 506 to 632 (Table S1). In the post-mineralization, the Stage 3 veins are composed abundantly of gangue minerals of quartz and calcite (Fig. S2d).

Alteration

Alteration zones along the 1800085mN section can be divided into 2 main phases (Fig. 5a) including quartz-adularia (silicic alteration) and adularia-quartz-illite-calcite-chlorite (phyllic alteration) zones. The presence of the quartz-adularia zone is confined to the proximity (< few meters) of veins, stockworks, and breccias in ore zones. The quartz-adularia zone (silicic alteration zone) is composed of quartz and adularia assemblage as confirmed by XRD pattern (Fig. 5b). Quartz and microcrystalline quartz replace and fill the groundmass and/or matrix of rocks (Fig. 5d and e). Adularia occurs commonly as euhedral grain in quartz veins with open space-filling features (Fig. 5e) as well as in wallrocks. The adularia-quartz-illite-calcite-chlorite zone (phyllic alteration) develops at the distal from the ore zone, and this alteration is pervasively formed in the wallrocks at the B prospect. XRD pattern obtained from the representative sample from phyllic alteration zone is shown in Fig. 5c, confirming such alteration mineral assemblage. The petrographic study suggests that quartz and adularia are significantly present in the silicic alteration zone (Fig. 5d and e), whereas illite and chlorite occur as replacement of feldspar minerals such as K-feldspar and plagioclase and mafic minerals such as hornblende, respectively (Fig. 5f and g).

DISCUSSION

Stratigraphic correlation

In order to understand the district-scale lithological control of the Au-Ag mineralization in the Chatree deposit, the volcanogenic sedimentary unit (Unit 1), polymictic mafic-intermediate breccia unit (Unit 2), and porphyritic andesite unit (Unit 3) in the host rock succession of the B prospect are stratigraphically correlated with those of the Chatree deposit [4, 7] and Suwan prospect [10, 26] (Fig. 6). The correlations indicate that the host rock successions between the B prospect and the Chatree deposit are similar, but the fiamme breccia unit is absent at the B prospect. This may suggest that the erosional level at B prospect is deeper than the Chatree deposit area, and it does not mean that the fiamme breccia unit is not deposited at the B prospect area as the unit is widespread to the east of the prospect (Fig. S1c).

For the lithological control of the gold-silver mineralization, it is found that the ore zones were selectively emplaced within the whole volcanogenic sedimentary unit (Unit 1) and upper polymictic mafic-intermediate breccia unit (Unit 2) at the B prospect, whereas at the Chatree deposit, they dominantly occurred in the entire volcanogenic sedimentary and polymictic mafic-intermediate breccia units. At the Suwan prospect, it is reported that polymictic mafic-intermediate breccia unit (Unit 2 of the B prospect) was absent and ore zones were dominantly hosted in the monomictic plagioclase-phyric andesite breccia unit [10], which corresponds to the Unit 3 of the B prospects. On the other hand, the fiamme breccia unit and coherent rocks including plagioclase-phyric andesite and hornblende-plagioclase-phyric andesite were unmineralized.

Gold mineralization

The textural features of gold-bearing veins/veinlets and stockworks in the B prospect include crustiform, colloform, and comb textures (Fig. S2b and c) which are similar to those found at the Chatree deposit. Such vein textures are typical feature of open space-filling veins [24]. Thus, it may indicate that the Au-Ag mineralization at the B prospect is formed by

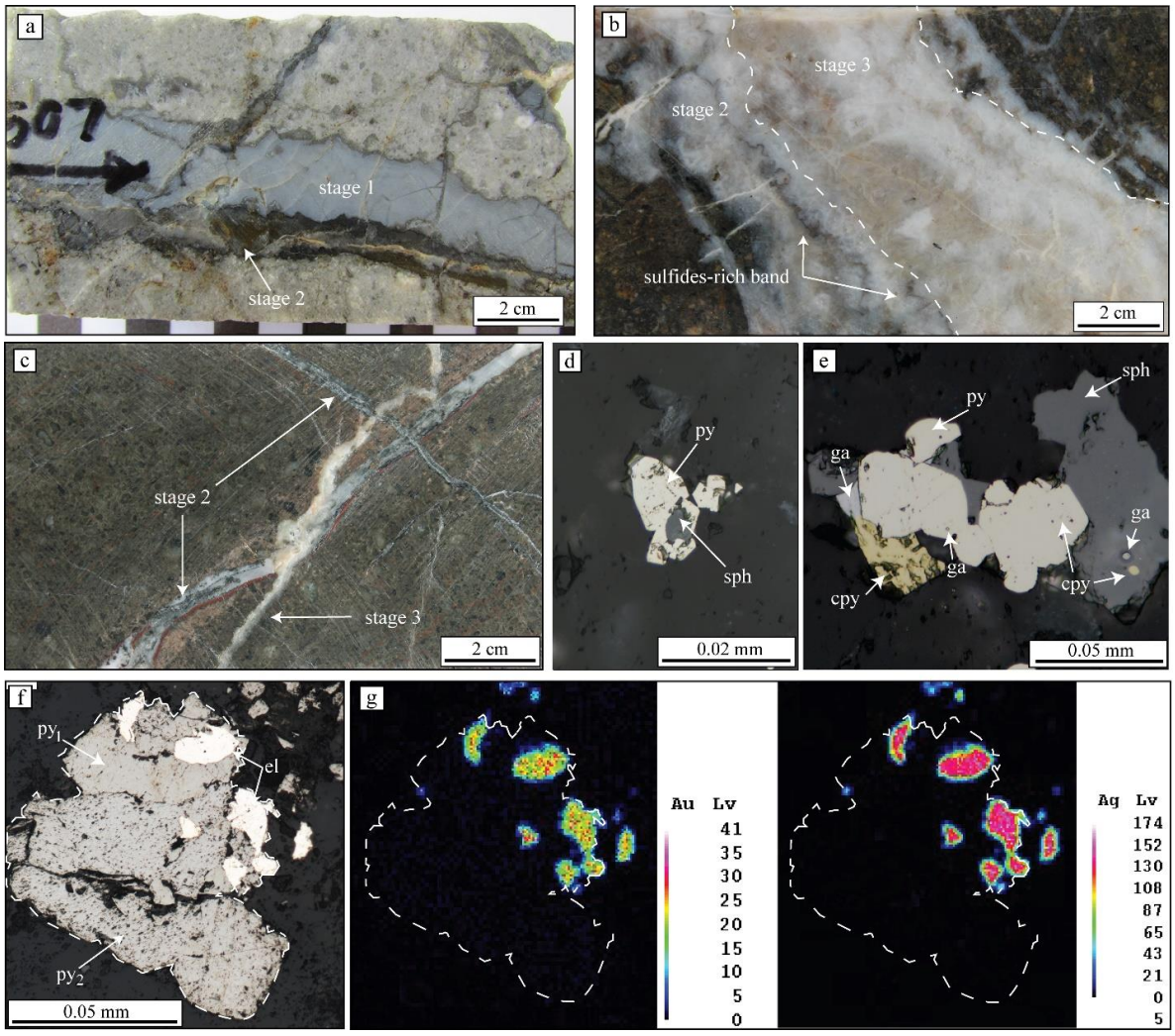

Fig. 4 Characteristics of mineralization and ore minerals of the B prospect. (a) Photograph of grey quartz-pyrite vein (Stage 1). (b) Photograph of quartz-chlorite-calcite-sulfide-electrum vein (Stage 2) showing sulfide-rich band and quartz-calcite vein (Stage 3). (c) Photograph of veinlets showing quartz-chlorite-calcite-sulfide-electrum vein (Stage 2) crosscut by quartz-calcite vein (Stage 3). (d) Photomicrograph of sphalerite occurrence as inclusion in pyrite. (e) Photomicrograph showing chalcopyrite, galena, and sphalerite associated with pyrite. Small chalcopyrite and galena occurrences as inclusions in pyrite and sphalerite. (f) Photomicrograph of gold-bearing vein showing electrum inclusion in pyrite. (g) EPMA mappings of pyrite and electrum showing high contents of Au and Ag in electrum. Abbreviations; py = pyrite, py1 = clean pyrite, py2 = porous pyrite, sph = sphalerite, cpy = chalcopyrite, and gl = galena.

hydrothermal fluids (< 1 km deep from surface) as also discussed and evidenced in [4] for the Chatree deposit. Salam [5] demonstrated from oxygen isotope data of the mineralized veins that the ore-forming hydrothermal fluids at the Chatree deposit were mixture of magmatic fluid and meteoric water. Therefore, the NNW-SSE trending fault zone hosting the Au-Ag mineralization at the B prospect as well as Chatree deposit and Suwan prospect is interpreted to be a deep-seated fault which can be connected to the magma source at deep and thus hydrothermal fluids can be migrated upwards along the fault.

It is also be pointed out that the mineralized veins/veinlets and breccias at the B prospect as well as Chatree deposit and Suwan prospect are exclusively hosted in the permeable rocks (i.e., volcanogenic sedimentary rock, sand-matrix polymictic breccia, lithic-rich fiamme breccia, polymictic mafic-intermediate breccia, and monomictic plagioclase-phyric andesite breccia) rather than impermeable rocks such as coherent volcanic rock and fiamme breccia. This may postulate that physical characteristic of host rocks such as permeability is also a key factor for hosting the Au-Ag mineralization at the B prospect, Suwan prospect,

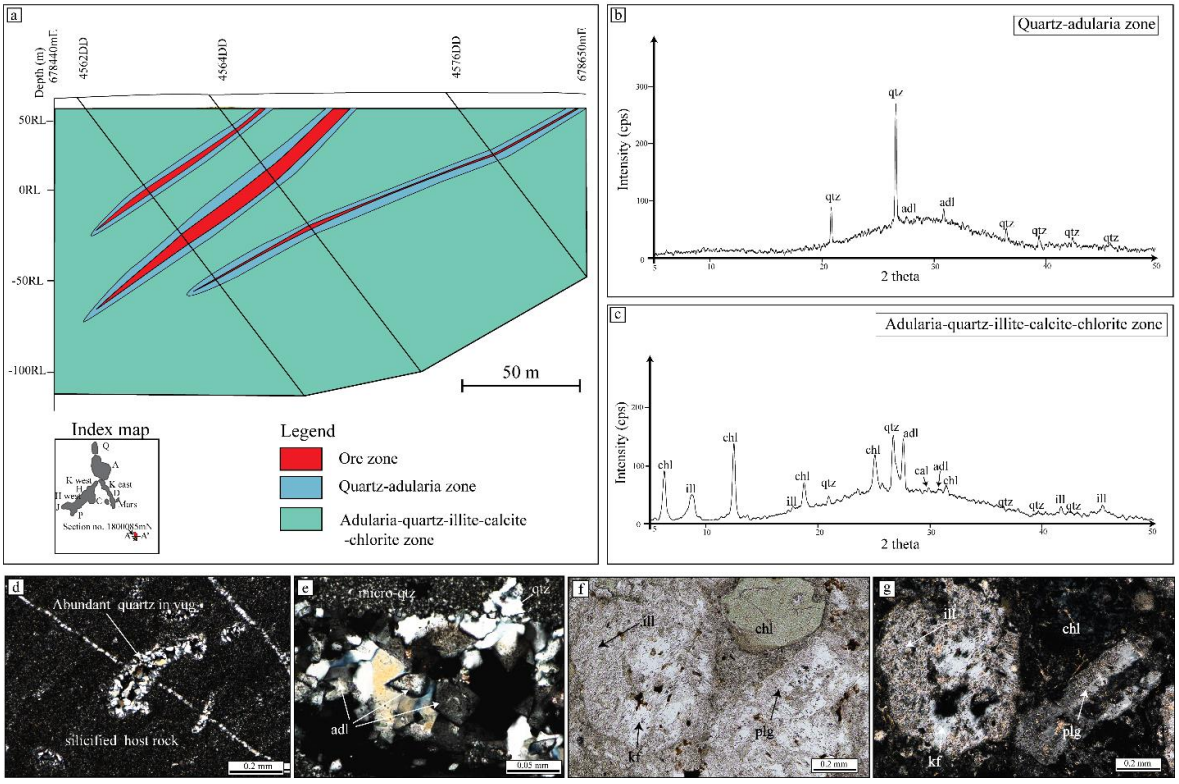

Fig. 5 (a) Alteration zones along the cross-section 1800085mN of the B prospect. (b) Representative XRD pattern of quartz-adularia zone. (c) XRD pattern of the representative sample from the adularia-quartz-illite-calcite-chlorite zone. (d) Photomicrograph of quartz-adularia zone showing abundant quartz filling open-space in the texture and replacing the matrix. (e) Photomicrograph of adularia in quartz-adularia zone showing rhombohedral crystal shape. (f) Photomicrograph of adularia-quartz-illite-calcite-chlorite zone showing alteration mineral assemblage enriched in illite and chlorite (PPL). (g) same as (f) in XPL. Abbreviations; qtz = quartz, adl = adularia, kf = K-feldspar, plg = plagioclase, chl = chlorite, ill = illite, and cal = calcite.

and Chatree deposit.

The nature and chemistry of ore-forming fluid in magmatic-hydrothermal systems normally reflect the formation of ore mineral assemblages in the veins, particularly sulfide minerals. The ore minerals of the B and Suwan prospects are lesser varying of sulfide contents compared to those of the Chatree deposit as they only include pyrite, chalcopyrite, sphalerite, and galena. In contrast, the Chatree deposit contains more variable ore minerals such as tetrahedrite, native silver, argentite, acanthite, boulangerite, pyrargyrite, arsenopyrite, and tetrahedrite. Furthermore, it is noted that sulfide minerals in the mineralized veins of B prospect as well as the Suwan prospect tend to be smaller in size than those in the Chatree deposit. These suggest that the gradients and extents of physico-chemical conditions of ore-forming fluids are much higher at the Chatree deposit, implying that the deposit is formed at the center of the epithermal system (feeder zone), whereas the Au-Ag mineralization of the B and Suwan prospects is interpreted to have occurred at the peripheral parts of the system.

For fineness values, the B prospect and Suwan prospects are confined to narrower ranges of 506–632 and 400–680 [10], respectively (Fig. 7). On the other hand, the Chatree deposit is variable in fineness ranges for each ore lens (e.g., 406 to 619 at A lens, 29 to 722 at K-east lens, and 6 to 581 at Q lens) that can be combined as a range of 6 to 722 [4]. These ranges indicate that they are broadly compatible with a range of epithermal Au-Ag deposits in the world [27] and such lower fineness values are considered the lower temperature of ore depositional environment compared to deposits in other styles (Fig. 7).

Alteration of B prospect

Results of this study identified 2 alteration types at the B prospect (i.e., quartz-adularia and adularia-quartz-illite-calcite-chlorite zones). At the Chatree deposit, Salam [4] reported that there is propylitic alteration which is composed of chlorite-calcite ± epidote assemblage in addition to the silicic (quartz-adularia) and phyllic (adularia-quartz-illite-calcite-chlorite) alteration phases. It is also recognized that the propylitic

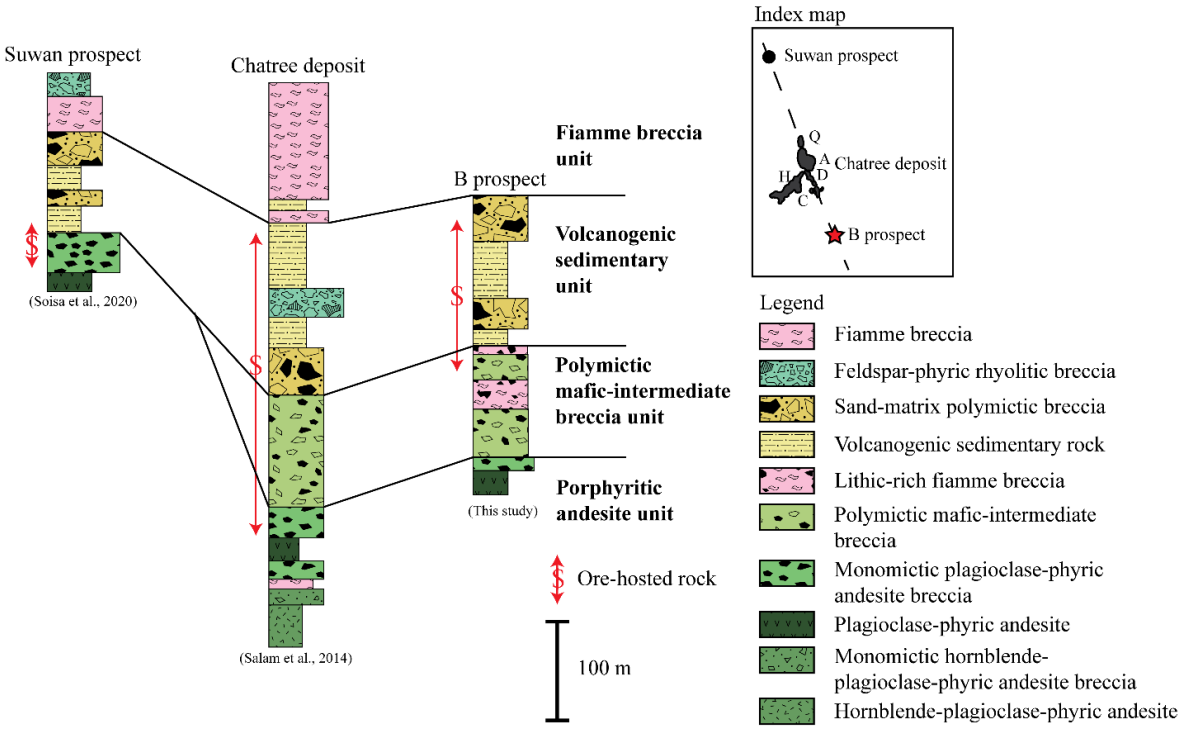

Fig. 6 Stratigraphic correlation between B prospect, Chatree deposit, and Suwan prospect.

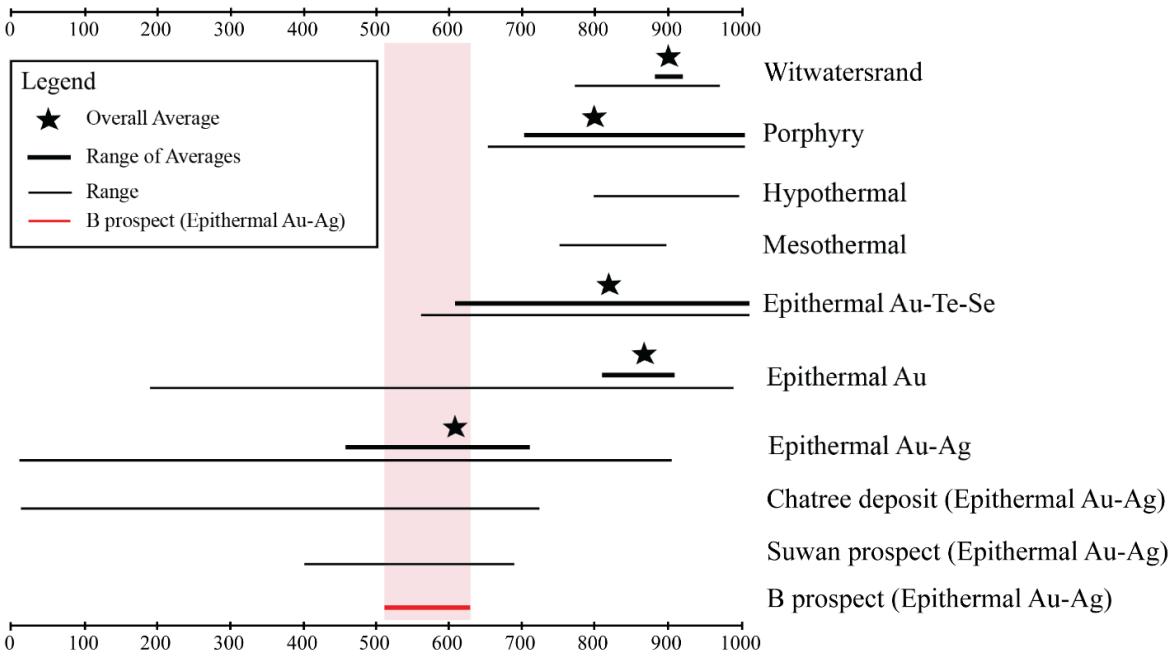

Fig. 7 Comparison diagram of fineness value of B prospect, Suwan prospect, and Chatree deposit with other mineral deposit styles (Modified from [27]).

alteration develops at the most distal part to the ore zone in the Chatree deposit at approximately > 200 m from ore zone as evidenced at the A ore lens [4]. This suggests that propylitic alteration can also be developed at the B prospect, but it was not observed at the B prospect in this study as locations of the investigated drill holes are restricted to the proximity to the ore zones.

The presence of adularia in the mineralized veins and altered wallrocks strongly supports that the B prospect is a low sulfidation epithermal deposit style [28] as hydrothermal fluids of low sulfidation epithermal deposits are produced by alkaline and moderate pH fluid, which can induce the deposition of adularia [29].

CONCLUSION

This study is conducted to investigate the geology, mineralization, and alteration of the B prospect which is one of the satellite systems of the Chatree deposit. The key conclusions are: (a) the geological setting of B prospect consists of 3 main rock units: volcanogenic sedimentary unit (Unit 1), polymictic intermediate breccia unit (Unit 2), and porphyritic andesite unit (Unit 3); (b) the main Au-Ag mineralization is the quartz-chlorite-calcite-sulfide-electrum veins/veinlets and stockworks; (c) the Au-Ag bearing veins are predominantly hosted by Unit 1 and 2 (permeable rocks), while the impermeable rocks are barren in mineralization; (d) the mineralized veins have distinct vein textures such as crustiform, colloform, comb, and banded features; gold occurs in the sulfide-rich black band; (e) alteration phases in the B prospect are composed of 2 main zones: Quartz-adularia (silicic alteration) and adularia-quartz-illite-calcite-chlorite (phyllic alteration) zones; (f) B prospect is defined as a low-sulfidation epithermal Au-Ag deposit representing a peripheral part of a large epithermal system centered at the Chatree deposit; and (g) the emplacement of the Au-Ag mineralization is principally controlled by the NNW-SSE trending fault which plays a key role in the upward migration of ore-forming fluids.

Appendix A. Supplementary data

Supplementary data associated with this article can be found at http://dx.doi.org/10.2306/scienceasia1513-1874.2022.142.

Acknowledgements: This research was financially supported by the CU Graduate School Thesis Grant. A great thank is extended to Akara Resources Public Co., Ltd. for allowing us to collect drill core samples and publish the results of this study. The authors also thank Mr. Weerasak Lunwongsa for his assistance with the ore lens location and data collection and Mr. Phuriwit Sangsiri of Akara Resources Public Co., Ltd. for his help to improve the manuscript.

REFERENCES

1. Kamvong T, Khin Zaw (2009) The origin and evolution of skarn-forming fluids from the Phu Lon deposit, northern Loei Fold Belt, Thailand: evidence from fluid inclusion and sulfur isotope studies. *J Asian Earth Sci* **34**, 624–633.
2. Khin Zaw, Meffre S, Lai CK, Burrett C, Santosh M, Graham I, Manaka T, Salam A (2014) Tectonics and metallogeny of mainland Southeast Asia: a review and contribution. *Gondwana Res* **26**, 5–30.
3. Rongkhapimonpong P (2015) Characteristics of vein related to high grade gold mineralization from eastern A pit of the Chatree gold deposit, Changwat Phichit and Phetchabun, Thailand. MSc thesis, Chulalongkorn Univ, Thailand.
4. Salam A (2013) A geological, geochemical and metallogenic study of the Chatree epithermal deposit, Phetchabun Province, central Thailand. PhD thesis, Univ of Tasmania, Australia.
5. Salam A, Khin Zaw, Meffre S, Golding S, McPhie J, Suphanathi S, James R (2008) Mineralisation and oxygen isotope zonation of Chatree epithermal gold-silver deposit, Phetchabun Province, central Thailand. In: *Proceeding of PACRIM 2008, The Pacific Rim: Mineral Endowment, Discoveries & Exploration Frontiers*, Queensland, Australia.
6. Salam A, Khin Zaw, Meffre S, James R, Stein H (2007) Geological setting, alteration, mineralization and geochronology of Chatree epithermal gold-silver deposit, Phetchabun Province, central Thailand. In: *Proceedings of Ores and Orogenesis Symposium*, Arizona, USA.
7. Salam A, Khin Zaw, Meffre S, McPhie J, Lai CK (2014) Geochemistry and geochronology of the Chatree epithermal gold-silver deposit: Implications for the tectonic setting of the Loei Fold Belt, central Thailand. *Gondwana Res* **26**, 198–217.
8. Tangwattananukul L, Ishiyama D (2018) Characteristics of Cu-Mo mineralization in the Chatree mining area, central Thailand. *Resour Geol* **68**, 83–92.
9. Tangwattananukul L, Ishiyama D, Matsubaya O, Mizuta T, Charusiri P, Sato H, Sera K (2014) Characteristics of Triassic epithermal Au mineralization at the Q prospect, Chatree mining area, central Thailand. *Resour Geol* **64**, 167–181.
10. Soisa T (2019) Geology and mineralization characteristics of epithermal gold, Suwan prospect, Changwat Phitsanulok. MSc thesis, Chulalongkorn Univ, Thailand.
11. Gemell Mining Engineers (2013) *Technical Review of the Chatree Gold Project*, Gemell Mining Services Proprietary Limited. Australia.
12. Metcalfe I (1984) Stratigraphy, paleontology and paleogeography of the carboniferous of Southeast Asia. *Mém Soc Géol France* **147**, 107–118.
13. Metcalfe I (2009) Late Palaeozoic and Mesozoic tectonic and palaeogeographical evolution of SE Asia. *Geol Soc Spec Publ* **315**, 7–23.
14. Sone M, Metcalfe I (2008) Parallel Tethyan sutures in mainland Southeast Asia: New insights for Palaeo-Tethys closure and implications for the Indosinian orogeny. *C R Geosci* **340**, 166–179.
15. Kamvong T, Khin Zaw, Meffre S, Maas R, Stein H, Lai CK (2014) Adakites in the Truong Son and Loei fold belts, Thailand and Laos: genesis and implications for geodynamics and metallogeny. *Gondwana Res* **26**, 165–184.

16. Khositanont S (2008) Gold and iron-gold mineralization in the Sukhothai and Loei-Phetchabun Fold Belts. PhD thesis, Chiang Mai Univ, Thailand.
17. Rodmanee T (2000) Genetic model of Phu Thab Fah gold deposit Ban Huai Phuk Amphoe Wang Saphung Changwat Loei. PhD thesis, Chiang Mai Univ, Thailand.
18. Khin Zaw, Kamvong T, Khositanont S, Mernagh T (2011) Oxidized vs. reduced Cu-Au skarn formation and implication for exploration, Loei and Truong Son fold belts, SE Asia. In: *Proceedings of International Conference on Geology, Geotechnology and Mineral Resources of Indochina (GEOINDO 2011)*, Khon Kaen, Thailand.
19. Khin Zaw, Rodmanee T, Khositanont S, Ruamkid S (2008) Geology, mineralogy and genesis of Phu Thap Fah gold skarn deposit, Northeast Thailand. Implications for reduced gold skarn formation. In: *33rd International Geological Congress (IGC)*, Oslo, Norway.
20. Khin Zaw, Rodmanee T, Khositanont S, Thanasuthipitak T, Ruamkid S (2007) Geology and genesis of Phu Thap Fah gold skarn deposit, northeastern Thailand: Implications for reduced gold skarn formation and mineral exploration. In: *Proceeding of GEOTHAI'07 International Conference on Geology of Thailand: Towards Sustainable Development and Sufficiency Economy*, Bangkok, Thailand.
21. De Little J (2006) Geological setting, nature of mineralisation, and fluid characteristics of the Wang Yai prospects, central Thailand. BSc thesis, Univ of Tasmania, Australia.
22. Muller C (1999) Geochemistry, fluid characteristics and evolution of the French mine gold skarn system, eastern Thailand. BSc thesis, Univ of Tasmania, Hobart, Australia.
23. Dong G, Morrison G, Jaireth S (1995) Quartz textures in epithermal veins, Queensland; classification, origin and implication. *Econ Geol* **90**, 1841–1856.
24. Hedenquist JW, Arribas R (2017) Epithermal ore deposits: first-order features relevant to exploration and assessment. *Min Resour Disc* **1**, 47–50.
25. Marsden J, House I (1992) *The Chemistry of Gold Extraction*, Ellis Howood Ltd., New York, USA.
26. Soisa T, Salam A, Manaka T (2020) Stratigraphy and petrochemistry of volcanic rocks at Suwan Prospect, Phitsanulok Province, central Thailand. *Bull Earth Sci Thail* **12**, 30–48.
27. Morrison GW, Rose WJ, Jaireth S (1991) Geological and geochemical controls on the silver content (fineness) of gold in gold-silver deposits. *Ore Geol Rev* **6**, 333–364.
28. Dong G, Morrison G (1995) Adularia in epithermal veins, Queensland: morphology, structural state and origin. *Miner Deposita* **30**, 11–19.
29. Browne P (1978) Hydrothermal alteration in active geothermal fields. *Annu Rev Earth Planet Sci* **6**, 229–248.

Appendix A. Supplementary data

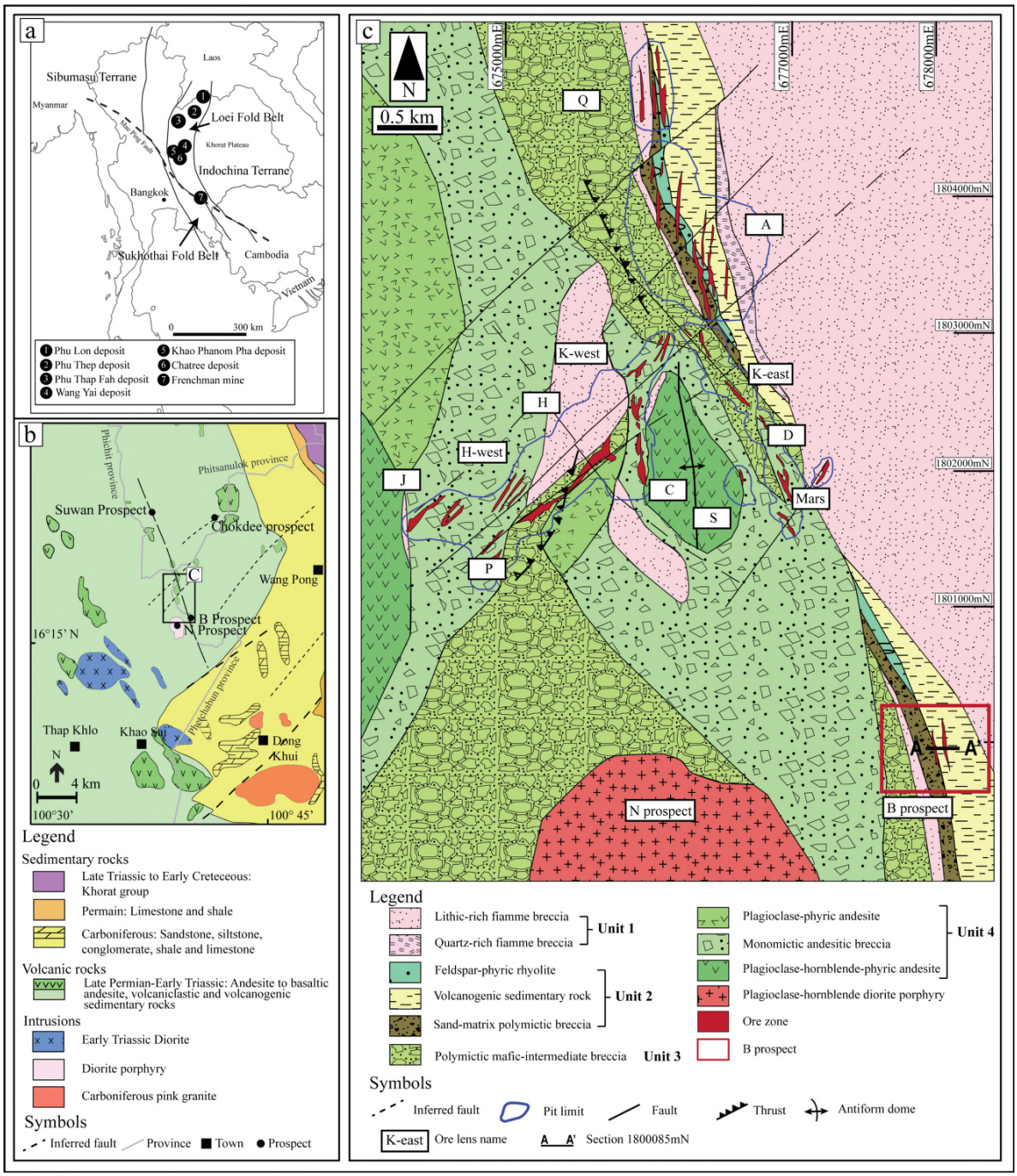

Fig. S1 (a) Tectonic map of Thailand showing the distribution of major gold-bearing deposits along Loei Fold Belt. (b) Regional geologic map of Chatree deposit and the surroundings showing location of the B prospect (Modified from [4]). (c) District-scale geologic map of Chatree deposit and the surroundings showing location of the B prospect relative to the Chatree gold mine (Modified from [4]).

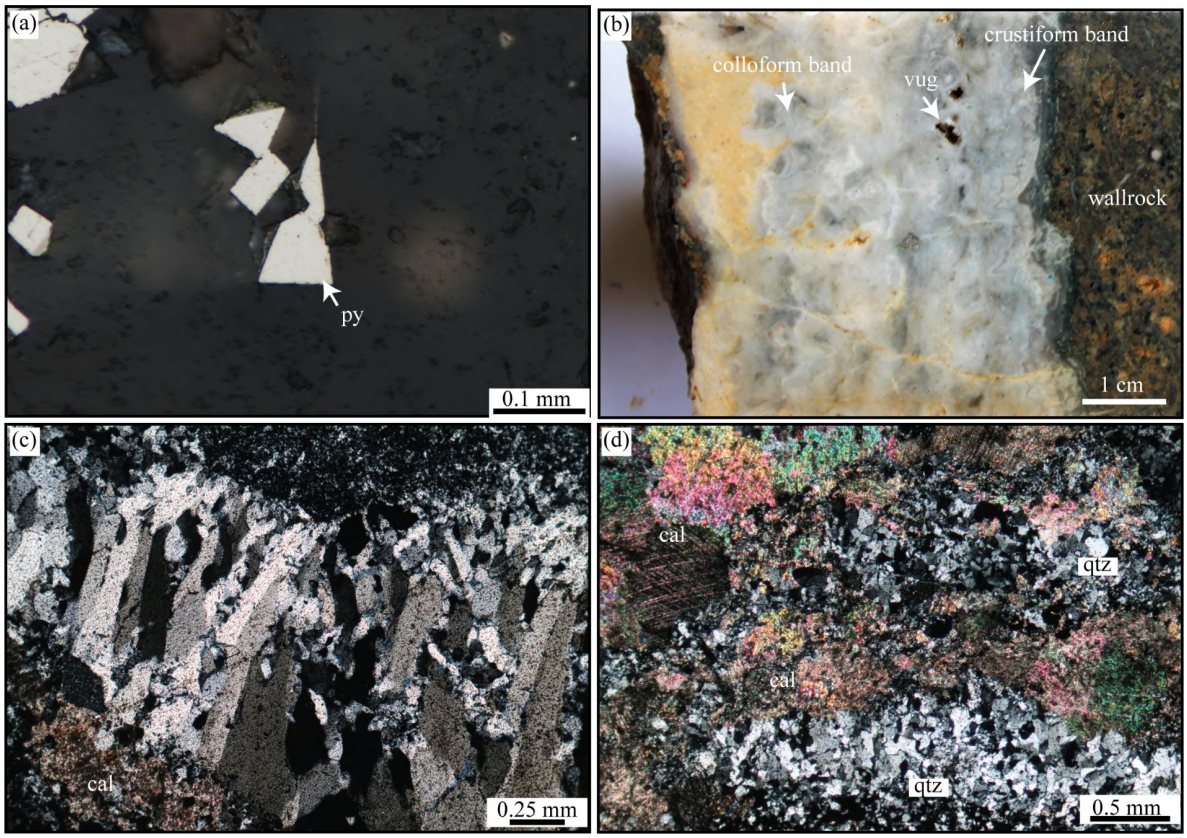

Fig. S2 (a) Photomicrograph of euhedral pyrite in Stage 1. (b) Photograph of the characteristics of quartz-chlorite-calcite-sulfide-electrum vein showing colloform-crustiform band. (c) Photomicrograph of textural feature of quartz vein in Stage 2 showing comb texture. (d) Photomicrograph of gangue minerals in quartz-calcite vein (Stage 3) showing quartz and calcite.

Table S1 Result of EPMA spot analysis of electrum.

No.	Spot ID	S	Pb	Cu	Fe	Zn	As	Au	Ag	Total	Fineness
1	B2-F-1	n.a.	n.a.	n.a.	0.05	n.a.	n.a.	59.37	37.26	96.68	614
2	B2-F-2	n.a.	n.a.	n.a.	n.a.	n.a.	n.a.	56.21	44.39	100.60	559
3	B2-F3-1	n.a.	0.05	n.a.	0.06	n.a.	n.a.	57.94	36.67	94.67	612
4	B2-F3-2	n.a.	n.a.	n.a.	n.a.	n.a.	n.a.	58.83	41.45	100.28	587
5	B2-F4-3	0.05	n.a.	n.a.	0.15	n.a.	n.a.	59.26	37.32	96.73	614
6	B2-F5-1	3.22	n.a.	0.12	3.36	n.a.	n.a.	50.26	37.35	90.97	574
7	B2-F6-1	n.a.	n.a.	n.a.	n.a.	n.a.	n.a.	50.51	49.26	99.77	506
8	B2-F6-2	n.a.	n.a.	0.07	n.a.	n.a.	n.a.	60.25	37.31	97.56	618
9	B2-F6-3	n.a.	n.a.	0.05	n.a.	n.a.	n.a.	60.07	36.50	96.57	622
10	B2-F7-1	0.09	n.a.	n.a.	0.06	n.a.	0.07	59.60	36.39	96.12	621
11	B2-F7-2	n.a.	n.a.	n.a.	n.a.	n.a.	n.a.	62.03	36.45	98.48	630
12	B2-F8-1	n.a.	0.06	n.a.	0.40	n.a.	n.a.	60.68	36.67	97.75	623
13	B2-F8-2	n.a.	0.05	n.a.	0.06	n.a.	n.a.	62.22	36.95	99.23	627
14	B2-F8-3	n.a.	n.a.	n.a.	0.10	n.a.	n.a.	63.39	36.84	100.33	632
15	B2-F9-1	0.07	0.05	n.a.	0.44	n.a.	n.a.	60.73	37.20	98.37	620
16	B2-F9-2	1.01	n.a.	n.a.	2.96	n.a.	n.a.	57.51	36.40	96.87	612
17	B2-F10-1	n.a.	n.a.	n.a.	0.36	n.a.	n.a.	60.75	37.54	98.65	618
18	B2-F10-2	n.a.	n.a.	n.a.	0.18	n.a.	n.a.	61.82	36.96	98.96	626
19	B2-F10-3	0.06	n.a.	0.08	0.35	n.a.	n.a.	62.04	36.49	98.88	630
20	B2-F11-1	0.49	n.a.	n.a.	2.24	n.a.	n.a.	50.33	46.10	98.67	522
21	B2-F11-2	0.94	n.a.	0.05	1.81	n.a.	n.a.	58.81	36.01	96.63	620
22	B2-F12-1	n.a.	n.a.	n.a.	0.28	n.a.	n.a.	62.10	36.82	99.20	628

n.a. = not available.

Table S1 Cont ...

No.	Spot ID	S	Pb	Cu	Fe	Zn	As	Au	Ag	Total	Fineness
23	B2-F12-2	n.a.	n.a.	n.a.	0.61	n.a.	n.a.	62.11	36.54	99.26	630
24	B2-F12-3	n.a.	n.a.	n.a.	0.29	n.a.	n.a.	60.83	36.89	98.01	622
25	B2-F13-1	n.a.	n.a.	n.a.	n.a.	n.a.	n.a.	56.75	36.51	93.26	609
26	B2-F13-2	0.10	n.a.	0.05	0.05	0.10	n.a.	57.70	36.82	94.67	610
27	B2-F14-1	n.a.	n.a.	n.a.	0.45	n.a.	n.a.	61.33	36.49	98.27	627
28	B2-F14-2	n.a.	n.a.	n.a.	0.07	n.a.	n.a.	62.39	37.27	99.73	626
29	B2-F14-3	n.a.	n.a.	n.a.	0.04	n.a.	n.a.	51.01	49.02	100.07	510
30	B2-F15-1	n.a.	n.a.	n.a.	0.66	n.a.	n.a.	60.37	36.79	97.82	621
31	B2-F16-1	0.15	0.14	n.a.	0.44	n.a.	n.a.	61.05	36.97	98.46	623
32	B2-F16-2	3.29	n.a.	n.a.	3.20	n.a.	n.a.	55.75	33.69	92.64	623
33	B2-F16-3	n.a.	n.a.	n.a.	0.13	n.a.	n.a.	59.51	36.67	96.31	619
34	B2-F18-1	n.a.	n.a.	n.a.	0.07	n.a.	n.a.	62.07	36.30	98.44	631
35	B2-F18-2	n.a.	n.a.	0.05	0.13	n.a.	n.a.	62.68	36.46	99.27	632
36	B2-F18-3	n.a.	n.a.	n.a.	1.19	n.a.	n.a.	60.70	36.15	98.04	627
37	B2-F19-3	n.a.	n.a.	n.a.	0.51	n.a.	n.a.	61.21	37.19	98.91	622
38	B2-F20-1	n.a.	n.a.	n.a.	0.05	n.a.	n.a.	60.92	36.95	97.92	622
39	B2-F20-2	n.a.	n.a.	n.a.	0.05	n.a.	n.a.	61.84	37.00	98.89	626
40	B2-F20-3	n.a.	0.05	n.a.	0.10	n.a.	n.a.	61.51	37.49	99.10	621
41	B2-F21-1	n.a.	0.08	n.a.	0.09	n.a.	n.a.	63.09	37.15	100.33	629
42	B2-F21-2	n.a.	n.a.	n.a.	0.07	n.a.	n.a.	62.89	37.57	100.53	626
43	B2-F21-3	n.a.	n.a.	n.a.	0.20	n.a.	n.a.	60.02	37.73	97.95	614
44	B2-F22-1	n.a.	n.a.	n.a.	n.a.	n.a.	n.a.	63.10	37.05	100.15	630
45	B2-F22-3	n.a.	n.a.	n.a.	0.16	n.a.	n.a.	61.96	36.94	99.06	626
46	B2-F23-1	n.a.	n.a.	0.08	n.a.	n.a.	n.a.	62.05	36.56	98.61	629
47	B2-F23-2	n.a.	n.a.	n.a.	0.09	n.a.	n.a.	61.40	36.97	98.46	624
48	B2-F24-3	0.06	n.a.	n.a.	1.14	n.a.	n.a.	59.74	36.79	97.67	619
49	B2-F25-2	0.05	0.06	n.a.	0.25	n.a.	n.a.	61.77	37.19	99.21	624
50	B2-F25-3	n.a.	n.a.	n.a.	0.06	n.a.	n.a.	59.71	37.25	97.02	616
51	B2-F26-1	n.a.	n.a.	n.a.	0.15	n.a.	n.a.	62.38	37.59	100.12	624
52	B2-F26-2	n.a.	n.a.	0.05	n.a.	n.a.	n.a.	62.58	37.10	99.68	628
53	B2-F27-1	n.a.	n.a.	0.05	0.08	n.a.	n.a.	62.46	37.09	99.63	627
54	B2-F27-2	n.a.	n.a.	n.a.	0.05	n.a.	n.a.	61.36	36.75	98.16	625
55	B2-F27-3	n.a.	n.a.	n.a.	n.a.	n.a.	n.a.	51.13	46.86	97.99	522
56	B2-F28-1	n.a.	n.a.	0.11	0.16	n.a.	n.a.	63.25	37.11	100.52	630
57	B2-F28-2	n.a.	n.a.	n.a.	n.a.	n.a.	n.a.	61.10	37.28	98.38	621
58	B2-F28-3	n.a.	n.a.	n.a.	n.a.	n.a.	n.a.	57.34	40.77	98.11	584
59	B2-F29-1	n.a.	n.a.	n.a.	n.a.	n.a.	n.a.	60.68	36.89	97.57	622
60	B2-F29-2	n.a.	n.a.	0.05	0.06	n.a.	n.a.	61.18	37.13	98.37	622
61	B2-F29-3	n.a.	n.a.	n.a.	n.a.	n.a.	n.a.	61.22	36.85	98.07	624
62	B2-F30-1	n.a.	n.a.	0.05	n.a.	n.a.	n.a.	61.06	37.16	98.22	622
63	B2-F30-2	n.a.	n.a.	n.a.	n.a.	n.a.	n.a.	59.11	36.24	95.35	620
64	B2-F30-3	n.a.	n.a.	0.07	0.38	n.a.	n.a.	61.60	37.20	99.18	623
65	B2-F31-1	n.a.	n.a.	n.a.	0.10	n.a.	n.a.	61.93	37.63	99.66	622
66	B2-F31-2	0.09	n.a.	n.a.	0.09	n.a.	n.a.	51.68	46.62	98.39	526
67	B2-F31-3	n.a.	n.a.	n.a.	n.a.	n.a.	n.a.	61.41	37.59	99.00	620
68	B2-F32-1	n.a.	n.a.	n.a.	n.a.	n.a.	n.a.	61.93	36.92	98.85	627
69	B2-F32-2	n.a.	n.a.	n.a.	n.a.	n.a.	n.a.	61.52	36.98	98.50	625
70	B2-F32-3	n.a.	n.a.	n.a.	0.07	n.a.	n.a.	60.58	36.66	97.31	623
71	B2-F33-1	n.a.	n.a.	n.a.	0.27	n.a.	n.a.	61.33	37.43	99.03	621
72	B2-F33-2	n.a.	n.a.	n.a.	0.15	n.a.	n.a.	60.02	37.20	97.37	617
73	B2-F33-3	n.a.	n.a.	n.a.	0.27	n.a.	n.a.	60.42	37.28	97.97	618
74	B2-F34-1	n.a.	n.a.	n.a.	0.58	n.a.	n.a.	51.78	40.96	93.32	558
75	B2-F34-2	n.a.	0.11	n.a.	0.13	n.a.	n.a.	58.71	37.82	96.66	608
76	B2-F34-3	n.a.	n.a.	n.a.	0.09	n.a.	n.a.	61.19	37.69	98.97	619
77	B2-F35-1	n.a.	0.07	n.a.	0.05	n.a.	n.a.	60.09	37.14	97.28	618
78	B2-F35-2	n.a.	0.08	n.a.	0.05	n.a.	n.a.	59.38	37.56	96.99	613
79	B2-F35-3	n.a.	n.a.	n.a.	0.08	n.a.	n.a.	60.41	37.92	98.41	614
80	B2-F36-1	n.a.	n.a.	n.a.	0.11	n.a.	n.a.	62.02	36.91	99.04	627
81	B2-F36-2	n.a.	n.a.	n.a.	0.07	n.a.	n.a.	61.47	37.61	99.15	620
82	B2-F36-3	n.a.	n.a.	n.a.	0.15	n.a.	n.a.	60.48	36.57	97.20	623
83	B2-F37-1	n.a.	n.a.	0.11	n.a.	n.a.	n.a.	63.08	36.98	100.06	630
84	B2-F37-2	n.a.	n.a.	n.a.	n.a.	n.a.	n.a.	63.37	36.97	100.34	632
85	B2-F37-3	n.a.	n.a.	n.a.	n.a.	n.a.	n.a.	61.09	37.97	99.06	617

n.a. = not available.